PAPER

Check for updates

Betaine host–guest complexation with a calixarene receptor: enhanced *in vitro* anticancer effect†

Sherif Ashraf Fahmy, [a] Fortuna Ponte,[b] Iten M. Fawzy,[c] Emilia Sicilia [b] and Hassan Mohamed El-Said Azzazy [*a]

p-Sulfonatocalix[*n*]arenes have shown excellent potential for accommodating chemotherapeutic drugs through host–guest complexation and enhancing their anticancer activity. Betaine has been reported to exert an anticancer effect at high concentrations. In order to increase its concentration in cancer cells, we have complexed it with *p*-SC4, which releases its content in an acidic environment typical of cancer tissue. In this work, a host–guest complex of the chemically stable, natural, and safe active methyl donor (betaine) and *p*-sulfonatocalix[4]arenes (*p*-SC4) was designed and characterized using ^{1}H NMR, UV, Job's plot analysis, DFT calculations, and molecular modeling for use in cancer therapeutics. The peak amplitude of the prepared host–guest complexes was linearly proportional to the concentration of betaine in the range of 1.0×10^{-5} M^{-1} to 2.5×10^{-4} M^{-1}. The reaction stoichiometry between *p*-SC4 and betaine in the formed complex was 1 : 1. The stability constant for the complex is 8.9×10^4 M^{-1} which corresponds to a complexation free energy of -6.74 kcal mol^{-1}. Complexation between betaine and *p*-SC4 was found to involve the insertion of the trimethylammonium group of betaine into the *p*-SC4 cavity, as supported by the experimental data. The complex displayed enhanced cytotoxic activities against breast adenocarcinoma cells (MCF-7) and cervical cancer cells (HeLa) compared to free betaine. In conclusion, the host–guest complexation of betaine with *p*-SC4 increases its concentration in cancer cells, which warrants further investigation for cancer therapy.

1. Introduction

Anomalies in genetic and epigenetic mechanisms cause cancer.[1] Typically, the epigenetic mechanisms involve various pathways responsible for gene expression regulation without manipulating the DNA sequence. DNA methylation, one of the epigenetic mechanisms, involves methylation of cytosine residues in cytosine–guanine (CG) pairs to form 5-methylcytosine.[1–3] Genomic deformations and loss of DNA integrity might occur due to hypomethylation of CG sites. This may lead to the initiation of specific proto-oncogenes, such as c-Myc, and the inactivation of tumor suppressors such as p16, resulting in the development and progression of tumor cells.[4] Under normal physiological conditions, optimal methylation profiles are maintained by achieving an equilibrium between DNA methylation and demethylation processes. However, many pathological events, including oxidative stress, inflammation, and cancer, disrupt this equilibrium.[5] Thus, the DNA methylation process has attracted attention as a target for cancer therapy because of its reversible nature.[6] In this regard, some studies reported the impact of diet and nutrients on DNA methylation *via* stimulating methyl donor production at specific CG sites.[7–9] This interface between nutrients and epigenetics (nutri-epigenomics) is a promising arena that may pave new avenues for future utilization of bioactive nutrients in cancer therapy. These include folic acid, vitamin B12, choline, and betaine which are considered essential methyl donors for DNA methylation.[3] Thus, they may exert preventive and curative effects against cancer.

Betaine, trimethylglycine, is a chemically stable, natural, and safe (at a dose up to 15 g per day) active methyl donor that supports the standard DNA methylation patterns.[10–12] Betaine is found in many dietary sources such as shrimps, wheat germ, wheat bran, spinach, and sugar beets.[12] Many studies reported betaine's ability to prevent and treat cancer, *in vitro*, *via* different mechanisms. One study reported the ability of betaine to induce tumor cell apoptosis *via* altering caspase proteins.[13] Betaine was found to affect pro-inflammatory cytokines levels, such as tumor necrosis factor-alpha inside various tumor cells.[14] Another study reported betaine's capability to stabilize multiple tumor suppressors and proto-oncogenes' methylation

aDepartment of Chemistry, School of Sciences & Engineering, The American University in Cairo, AUC Avenue, PO. Box 74, New Cairo 11835, Egypt. E-mail: sheriffahmy@ aucegypt.edu; hazzazy@aucegypt.edu; Fax: +20 2 2795 7565; Tel: +20 2 2615 2559

bDepartment of Chemistry and Chemical Technologies, University of Calabria, Arcavacata di Rende, 87036, Italy. E-mail: fortuna.ponte@unical.it; emilia.sicilia@ unical.it

cPharmaceutical Chemistry Department, Faculty of Pharmaceutical Sciences and Pharmaceutical Industries, Future University in Egypt, Cairo 12311, Egypt. E-mail: iten.mamdouh@fue.edu.eg

† Electronic supplementary information (ESI) available. See DOI: 10.1039/d1ra04614d

patterns and regulate their expression.[15] Researchers reported the cytotoxic activity of different betaine doses on human prostate cancer cells (DU-145).[16] However, high doses of betaine are required to exert its anticancer action.[17]

The use of various delivery vehicles to reformulate natural anticancer agents is a promising approach that may improve their uptake into target tumor cells while simultaneously providing a shield that protects these agents from degradation in the circulation.[18] Many studies reported the use of various delivery vehicles to accommodate several anticancer agents.[19–24] The host–guest complexation chemistry (macrocycles) has recently attracted much attention as promising drug delivery vehicles.[25,26] Many studies reported the possible use of supramolecular structures as hosts for different antineoplastic drugs to enhance their water solubility, chemical stability and improve their selective uptake into tumor cells.[26–29] Particularly, calix[n]arenes (n = 4, 6, and 8) signify a crucial class of macrocycles that have been widely utilized in drug delivery. Calixarenes are ideal host molecules formed of phenolic units linked by methylene bridges comprising an upper rim with *para*-substituent of a phenolic ring, a lower rim with a phenolic hydroxyl group, and a hydrophobic π electron-rich core cavity. This unique structure of calix[n]arenes permits their facile functionalization using sulfonate groups *via* their phenolic rings' *para*-position, forming the water-soluble derivative (>0.1 mol L^{-1}), *para*-sulfonatocalix[n]arenes.[26–29] *para*-Sulfonatocalix[n]arenes are nontoxic to human cells at *in vivo* doses up to 10^3 μg kg^{-1}. Furthermore, in aqueous media, *para*-sulfonatocalix[n]arenes demonstrated an ability to host different guest molecules in their cavities *via* inclusion complexation.[30,31]

In this study, the complexation between *p*-SC4 and betaine in an aqueous solution was studied for potential application in cancer therapeutics. The proposed complex has been characterized by UV, ^{1}H NMR spectroscopy, and computational studies. The stoichiometry and binding constant were computed utilizing Job's plot (continuous variation method). Density functional theory (DFT) calculations were carried out to characterize the structure of the host–guest adduct. Moreover, the anticancer activities of the complex against breast adenocarcinoma (MCF-7) and cervical cancer (HeLa) were studied.

2. Experimental and computational details

2.1. Reagents

Betaine and *para*-sulfocalix[4]arene, *p*-SC4, were obtained from BLD Pharmatech Co., Limited (Cincinnati, OH). Deuterium oxide and HPLC grade water were purchased from Sigma-Aldrich. Streptomycin, penicillin, fetal bovine serum, trichloroacetic acid (TCA), Dulbecco's Modified Eagle's Medium (DMEM), SRB, and tris(hydroxymethyl)aminomethane (TRIS) were purchased from Lonza (Basel, Switzerland).

2.2. Instrumentation

UV spectrophotometric measurements were carried out on a CARY 500 UV-vis-NIR Scan dual-beam spectrophotometer (Varian, Palo Alto, CA). ^{1}H NMR spectra were measured on a JEOL type GSX-270 or JNM-ECA 500II spectrometer (Jeol, Peabody, MA).

2.3. Cell viability assay

Breast adenocarcinoma (MCF-7) and cervical cancer (HeLa) were obtained from American Type Culture Collection (Manassas, VA). The cells were sustained in DMEM medium supplemented with streptomycin (100 mg mL^{-1}), penicillin (100 units per mL), and 10% heat-inactivated fetal bovine serum. Cells were incubated in 5% (v/v) CO$_2$ at 37 °C.

2.4. Sulforhodamine B colorimetric assay (SRB)

To investigate the cytotoxicity of the designed betaine/*para*-sulfocalix[4]arene, MCF-7 and HeLa cancer cell lines were treated with different concentrations of *p*-SC4, individual betaine, and B/*p*-SC4. The cell viability of either cancerous or non-cancerous cells was examined employing the SRB assay, and the IC$_{50}$ (in μg mL^{-1}) was calculated using our methods described previously.[28,29,32–34]

2.5. DFT calculations

All the electronic calculations were performed using the Gaussian 09 package[35] in the framework of the density functional theory (DFT). The geometries of the investigated host–guest complexes were fully optimized in water media employing the B97-D exchange and correlation functional.[36]

The geometry optimizations were performed using the double-zeta 6-31G(d,p) basis set for all the involved atoms, except for oxygen atoms, for which a diffuse function was included. The solvation effects were computed using the continuum solvation model based on density (SMD),[37] as implemented in Gaussian 09. To confirm the minimum character of the intercepted structures, vibrational frequency analysis was carried out at the same level of theory, and frequency calculations, within the harmonic approximation, were used to calculate the Gibbs free energies for the inclusion of betaine (G) into calixarenes (H).

The inclusion Gibbs free energies in solution ΔG_{sol}, in implicit water, was calculated as the difference between the free energy in solvent ($G_{\text{sol}}^{\text{HG complex}}$) of the complex and the free energies of the separated species in solvent ($G_{\text{sol}}^{\text{H}}$ and $G_{\text{sol}}^{\text{G}}$):

$$\Delta G_{\text{sol}}^{\text{HG complex}} = G_{\text{sol}}^{\text{HG complex}} - (G_{\text{sol}}^{\text{H}} + G_{\text{sol}}^{\text{G}})$$

Counterpoise correction calculations, as formulated by Boys and Bernardi[38] were carried out to estimate the Basis Set Superposition Error (BSSE).

The characterization of molecular interactions responsible for the formation of the betaine–*p*-SC4 adducts was performed using the theory of atoms in molecules (AIM) suggested by Bader,[38,39] using the AIMAll program.[40]

The analysis of the electron density $\rho(r)$ around the interacting species allows identification of the chemical bonding nature of the optimized geometries.

The values of $\rho(r)$ and its derivatives at the CPs (Critical Points; points where the gradient of the density is zero, $\nabla\rho(r) = 0$) provides information about the nature and the strength of the established interactions. To characterize the CPs, it is necessary to explore the second-order derivatives of $\rho(r)$. Only nine derivatives are possible, useful to generate a real and symmetric Hessian matrix of $\rho(r)$. The diagonalization of the matrix, using a unitary transformation, allows finding the corresponding eigenvalues (λ_n). CPs are marked by the rank ω and the signature σ, respectively. The rank of the diagonalized matrix is given by the number of non-zero eigenvalues (non-zero curvatures of $\rho(r)$ at the CPs). The signature of a CP, σ, is defined as the algebraic sum of the signs of the eigenvalues (signs of curvatures of $\rho(r)$ at the CPs). CP with $\omega = 3$ and $\sigma = +1$, corresponding to (3, +1) CP, has two positive curvatures, and ρ is a minimum at CP in the plane defined by their corresponding axes while at CP along the third axis, perpendicular to this plane, ρ is a maximum. The CP (3, −1), with $\omega = 3$ and $\sigma = -1$, highlights that electronic charge density is located within a chemical bond between the involved atoms. Such a point is called the bond critical point (BCP).

3. Results

3.1. H NMR spectroscopy

^{1}H NMR measurements carried out in D_2O were implemented to inspect the complexation between betaine and p-SC4. The ^{1}H NMR spectra for each of p-SC4, betaine, and 1 : 1 molar ratio mixture of p-SC4 and betaine are presented in Fig. S1A–C;† respectively. The ^{1}H NMR findings showed that the protons of betaine had exhibited remarkable upfield shifts upon adding p-SC4 (Table 1 and Fig. S1†) relative to those of the betaine alone. These shifts are attributed to the shielding effect of the aromatic rings of p-SC4. Previous studies reported the direct relationship between the degree of the chemical shift of a guest molecule's protons and their depth of penetration inside the hollow cavity of the host molecule, designating the formation of host–guest inclusion complexes.[28,29,41,42] The most significant upfield shift of ~0.58 ppm was observed for the protons of the methyl groups bonded to the quaternary ammonium head of betaine, H_c (Table 1 and Fig. S1†) showing that they possessed the most significant shielding effect. These indications suggest the

possible insertion of betaine inside the p-SC4 cavity through its N-terminal moiety. Moreover, the signals of the aryl and methylene bridge protons (H_a and H_b; respectively) of p-SC4, exhibited some chemical shifts upon betaine addition, which indicates the formation of host–guest inclusion complex (Table 1 and Fig. S1†).[27–29]

3.2. UV-vis spectroscopy

The formation of host–guest inclusion complexes between betaine and p-SC4, was investigated using UV-Vis spectroscopy.[27–29] The UV absorbance spectra of 0.2 mM betaine, 0.2 mM p-SC4, and a mixture comprising a mixture of 0.2 mM of each of betaine and p-SC4 in deionized water are presented in Fig. 1. Betaine exhibited weak absorbance across the wavelength range of 240–340 nm. The individual p-SC4 spectrum, conversely, showed remarkable absorption maxima at 277 and 284 nm. The spectrum of the mixture displays the merging of the two absorption maxima, distinctive to individual p-SC4, forming a new single peak at 282 nm. As previously reported, this is attributed to the formation of the betaine/p-SC4 inclusion complex.[27–29] The UV absorbance spectra of mixtures comprising increasing betaine concentrations (ranging from 0.01–0.25 mM) and a fixed concentration (0.2 mM) of p-SC4 in all mixtures were measured. A gradual merging of the pair of absorption maxima, distinctive of the individual p-SC4, was observed along with a remarkable hyperchromic shift, correlated with the increase of betaine concentration in the range of 0.01–0.25 mM (Fig. S2†).

The hyperchromic shift observed with increasing betaine concentrations was obtained by dividing the zero-order spectra of the prepared mixtures by the spectrum of p-SC4 where the first derivative of the ratio spectra was computed using a scaling factor of 10 and $\Delta\lambda = 4$ nm.[27–29] The values of the peak amplitudes of the first derivative of the ratio spectra for the mixtures were then measured at 264 nm. A plot of the obtained peak amplitudes and the equivalent concentrations of betaine is presented in Fig. 2. The idyllic linear relationships illustrated in Fig. 2 proposed that the hyperchromic shift detected in betaine/p-SC4 is due to the formation of host–guest inclusion complex between betaine and p-SC4.

The stoichiometry and the stability constants of the host–guest inclusion complex were examined using Job's plot (the method of continuous variation) utilizing the derivative ratio method as described previously.[27–29] From Job's plots, we noticed that the maximum amplitudes were spotted at molar fractions of 0.5, signifying a host–guest inclusion complex stoichiometry of 1 : 1 for betaine/p-SC4. A normalized form of this Job's plot for betaine/p-SC4, where each amplitude value, S, was divided by the corresponding maximum amplitude, S_{max}, is depicted in Fig. 3. The stability constant of the betaine/p-SC4 inclusion complex computed employing methods detailed previously[27–29] was 8.9×10^4 M^{-1} which corresponds to the complexation free energy of -6.74 kcal mol^{-1}. This value agrees well with the stability constants (0.01×10^3 to 1.7×10^5 M^{-1}) previously reported for host–guest inclusion complexes proposed to be applied in drug delivery. Many of them showed

Table 1 Detected shielding (ppm) for allocated protons in p-SC4, betaine, and 1 : 1 M ratio mixture in D_2O. Proton labels are demonstrated in Fig. S1[a]

Proton signals	Individual molecules	1 : 1 molar ratio
H_a	7.39	7.52
H_b	3.84	3.65
H_c	3.08	2.50
H_d	3.71	3.64

[a] H_a and H_b represent the aryl and methylene bridge protons in p-SC4, respectively. H_c and H_d represent the methyl and methylene protons in betaine, respectively.

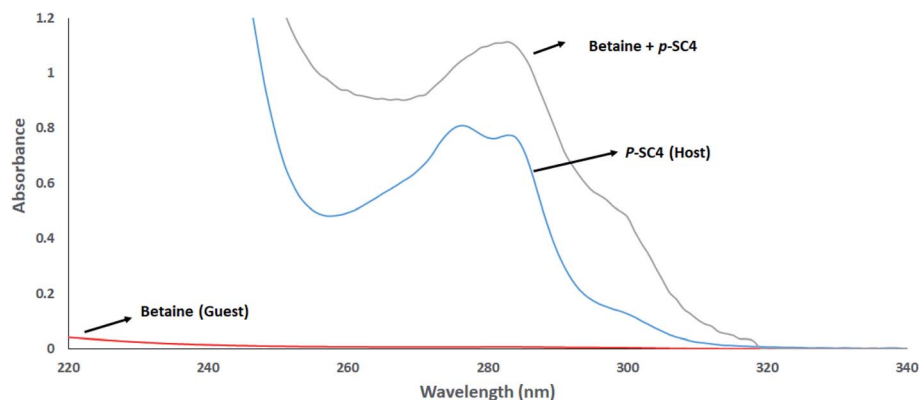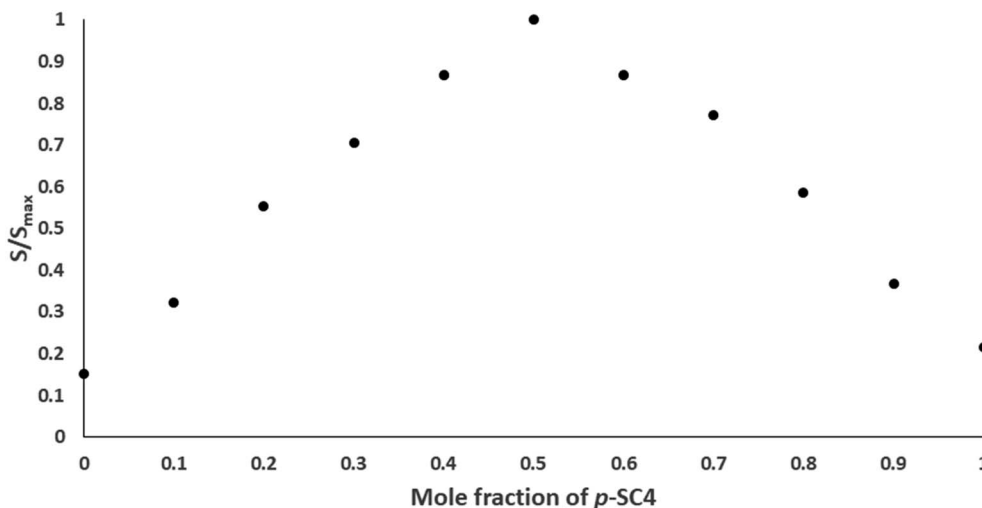

Fig. 3 Normalized Job's plot where each of the amplitude values, *S*, of the first derivative ratio spectra peaks were divided by the maximum amplitude, S_{max}, are plotted against the mole fraction of the equivalent *p*-SC4 molar fraction.

Table 2 *In vitro* cytotoxic activities of *p*-SC4, betaine, and betaine/*p*-SC4 against MCF-7 and HeLa. The treatment period was 72 h[a]

Cells	*In vitro* cytotoxic activity (IC_{50} in μg mL^{-1})		
	p-SC4	Betaine	Betaine/*p*-SC4
MCF-7	>300	>220	1.6 ± 1.4
HeLa	>300	>220	3.3 ± 1.1

[a] Data represent the mean ± standard deviation of triplicate.

to selectively release anticancer drugs in a controlled pH-dependent mechanism.[28,29,55–57] This would focus the action of betaine as a methyl donor on cancer cells while exerting minimal nonspecific effects on normal cells. Betaine's anticancer activity is attributed to its ability to regulate tumor necrosis factor-alpha (TNF-α) inside various tumor cells and stabilize multiple tumor suppressors and proto-oncogenes' methylation patterns and hence regulate their expression. Also, betaine induces apoptotic pathways *via* caspase 3 signaling leading to the prevention of tumor growth.[14–16] Thus, this work

highlights the potential use of the betaine/*p*-SC4 complex for targeting cancer cells.

3.4. DFT calculations

The most stable structure of the *para*-sulfonato-calix[4]arene (*p*-SC4), as shown in Fig. 4, assumes a typical cone-shaped conformation stabilized by intramolecular H-bond, between the OH groups, in the lower rim. The *p*-SC4 is characterized by upper and lower rim distances of 8.207 Å and 5.240 Å, respectively. As previously reported, such a conformation suggests that the preferred entrance channel of guest molecules is that from the side of the upper rim.[29]

The inclusion of guest molecules in the host cavity, as was shown recently, can be predicted based on their volumes. For *p*-SC4, the inner cavity volume results to be 652 Å^3, while betaine has a volume of 114 Å^3. Based on the calculated volumes, the penetration of betaine inside the *p*-SC4 receptor, in principle, could take place, even if, in the formation of the host–guest inclusion compounds, several aspects must be taken into consideration as illustrated below.
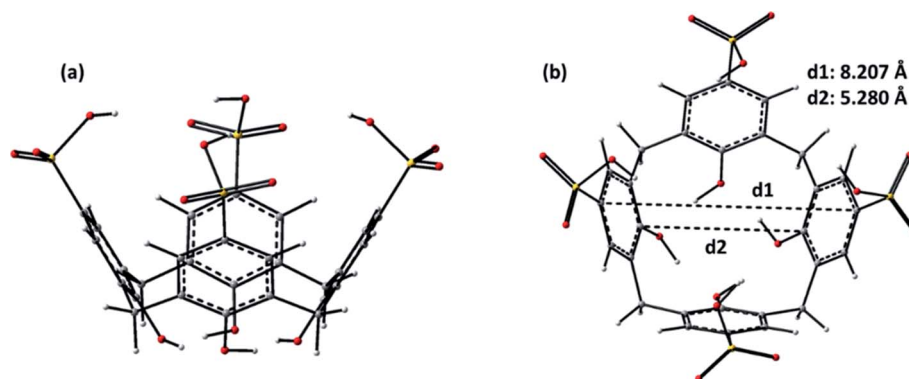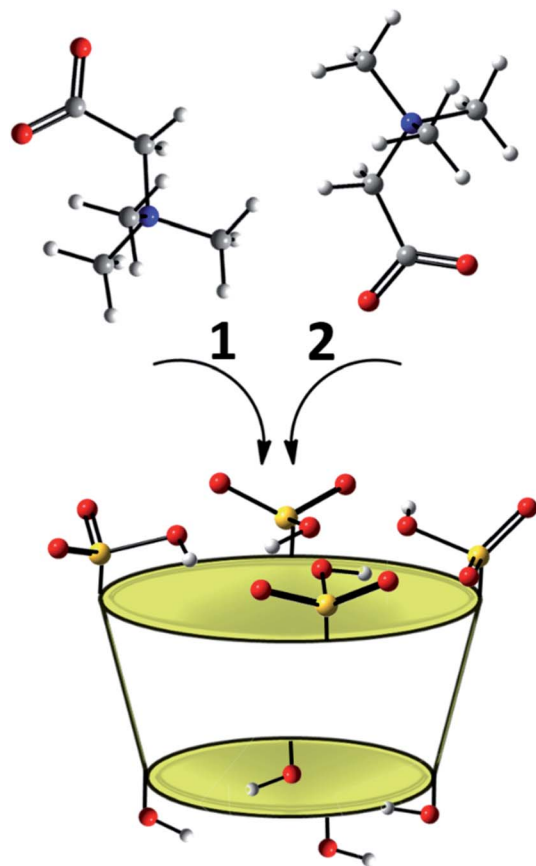

Fig. 4 B97-D optimized structures of *p*-SC4: (a) side view and (b) top view. Upper (d_1) and lower (d_2) rim diameters of the calixarene are reported.

Table 3 Electron density values $\rho(r)$, Laplacian of electron density $\nabla^2\rho(r)$, for $1_{H\text{-}G}$ and $2_{H\text{-}G}$ complexes. All data are in a.u.

Conformation	BCP	ρBCP	$\nabla^2\rho$BCP
$1_{H\text{-}G}$	1	0.011	0.750
	2	0.024	0.138
$2_{H\text{-}G}$	1	0.054	0.138
	2	0.054	0.148
	3	0.025	0.077
	4	0.054	0.136

Scheme 1 Computationally investigated inclusion modes of betaine into the p-SC4 cavity.

The potential insertion modes, computationally explored, of the betaine into the host molecule are reported in Scheme 1. In particular, the betaine can assume two different possible orientations with respect to the p-SC4 macrocycle. In the arrangement labelled as **1**, the positively charged trimethylammonium group points inwards the host cavity, and the carboxylate group points outwards, while the disposition in

which the carboxylate group points towards the inside of the cavity and the trimethylammonium group is outwardly oriented is labelled as **2**.

The optimized geometries obtained for the formation of host–guest complexes (or adducts) between betaine and p-SC4 receptor are illustrated in Fig. 5. In the same figure, the most relevant distances together with the highlighted Bond Critical Point (BCPs) and the values of the complexation free energies are reported. The energy of complexation was calculated, including the effect of basis set superposition error (BSSE) and entropy change corrections in the solution.

In the optimization process, any constraints were imposed. In the intercepted structure labelled as $1_{H\text{-}G}$, the betaine penetrates deeper into the host cavity, maximizing the electrostatic interactions. In particular, in this insertion complex, the quaternary ammonium group is located inside the p-SC4 cavity, while the carboxylate group points towards the upper ring establishing hydrogen bond interactions with the protonated oxygen atoms of the two closest sulfonate groups. The data computationally obtained for this inclusion complex reflects the information coming from ^{1}H NMR analysis. The formation of this betaine/p-SC4 adduct leads to an energy gain compared to separate species, and the value of the calculated complexation free energy is -12.8 kcal mol^{-1}.

In the $2_{H\text{-}G}$ adduct, the betaine guest interacts with the cavity of the receptor through the carboxylate group of betaine, and the trimethylammonium group points outwards. In particular, the carboxylate group of the host interacts with all the sulfonate
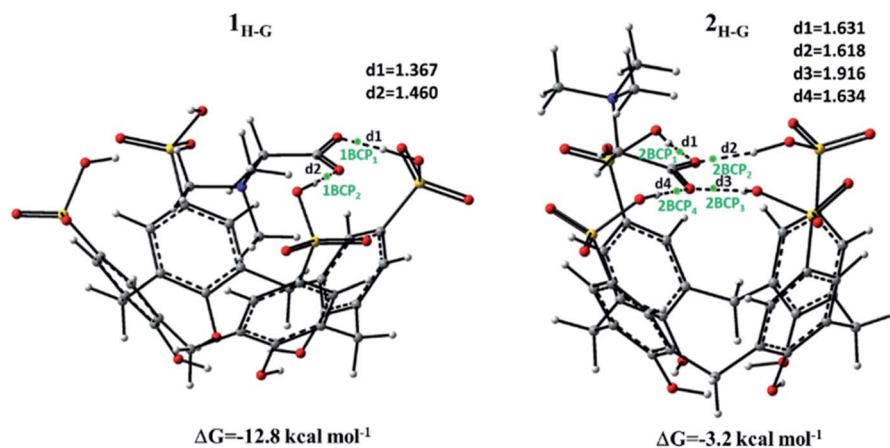

Fig. 5 B97-D optimized geometrical structures of $1_{H\text{-}G}$ and $2_{H\text{-}G}$ complexes are reported together with the most relevant geometrical parameter (Å), calculated complexation free energies, and BCPs present.

groups of the guest through intermolecular hydrogen bonds, causing the closure of the upper rim, whose diameter decreases by 0.537 Å. The free energy of complexation for the 2_{H-G} complex calculated to be −3.2 kcal mol^{-1} is smaller than the 1_{H-G} complex.

With the aim to investigate more in-depth the host–guest interactions, the AIM tool was used.[39,40] The electron density (ρ) value and its Laplacian $\nabla^2\rho(r)$ at the bond critical point (BCP) were estimated by AIM calculation to determine the nature and the strength of the interactions between the species forming both 1_{H-G} and 2_{H-G} complexes. In particular, for van der Waals interactions $\rho(r)$ is 10^{-3} a.u., while for hydrogen bonding $\rho(r)$ is ~10^{-2} a.u. or less. For both interactions, the corresponding Laplacian $\nabla^2\rho(r)$ is positive. Table 3 reports the results obtained from the AIM analysis.

In both complexes generated by the betaine guest and the calix p-SC4 host, the electron density values fall in the expected range for H-bonds, namely, 0.0102–0.0642 a.u.,[39] and for all the BCPs, the Laplacian sign is positive. The strength of these hydrogen interactions in the identified complexes is established by the highest positive values of the Laplacian.

As reported in Fig. 5, two BCPs, 1BCP1 and 1BCP2, respectively, are predicted for the 1_{H-G} complex. The value of Laplacian is larger for BCP1 than for BCP2, indicating a stronger interaction. In the 2_{H-G} complex, as shown in Fig. 5, four critical points indicated as 2BCP1, 2BCP2, 2BCP3, and 2BCP4 are established. All the BCPs correspond to hydrogen bonds and are defined by values of the Laplacian that are positive and of the same magnitude, except for BCP3 which is described by a smaller Laplacian value indicating a lower interaction. The formation of these H-bonds increases the stability of the adduct with respect to the separate species.

4. Conclusions

Betaine has been reported to exert an anticancer effect at high concentrations. To increase its concentration in cancer cells, a complex of betaine/p-SC4 has been designed, which releases its content in cancer cells (pH 5.5). Data from ^{1}H NMR, UV spectroscopy, Job's plot, and theoretical calculations supported the successful formation of the host–guest inclusion complex between p-SC4 and betaine in a 1 : 1 molar ratio. The stability constant of betaine/p-SC4 was computed to be 8.9×10^4 M^{-1}, which corresponds to the free energy of complexation of −6.74 kcal mol^{-1}. The stability of the prepared complex in an aqueous medium supports its application in cancer drug delivery. Both ^{1}H NMR spectroscopy and DFT calculations indicate that betaine was included within the cavity of p-SC4, and the complexation involves the insertion of the trimethyl-lammonium group of the guest into the host cavity. Data from the SRB assay showed that the IC$_{50}$ of betaine/p-SC4 was 1.6 ± 1.4 and 3.3 ± 1.1 μg mL^{-1} against MCF-7 and HeLa cells, respectively, compared to individual betaine, which exerted a negligible decline of cell viability.

In summary, the complexation between p-SC4 and betaine was thoroughly investigated experimentally and computationally. To the best of our knowledge, there are no reports on encapsulation of betaine in nanocarriers or supramolecular structures. A remarkable enhancement of the cytotoxic activities of betaine/p-SC4 was observed in two different cancer cell lines as compared to free betaine. This work presents a novel approach for delivering high betaine concentrations into cancer cells and supports the potential use of the designed complex as a possible effective supplement to cancer therapeutics.

Conflicts of interest

The authors declare no conflict of interest.

Acknowledgements

References

1 S. Biswas and C. M. Rao, *Pharmacol. Ther.*, 2017, **173**, 118–134.

2 G. S. Ducker and J. D. Rabinowitz, *Cell Metab.*, 2017, **25**, 27–42.

3 S. Zeisel, *Nutrients*, 2017, **9**, 445.

4 M. Kulis, A. C. Queiros, R. Beekman and J. I. Martin-Subero, *Biochim. Biophys. Acta*, 2013, **1829**, 1161–1174.

5 C. X. Song and C. He, *Genome Biol.*, 2012, **13**, 173.

6 A. Ghobadi, J. Choi, M. A. Fiala, T. Fletcher, J. Liu, L. G. Eissenberg, C. Abboud, A. Cashen, R. Vij, M. A. Schroeder, *et al.*, *Leuk. Res.*, 2016, **49**, 1–6.

7 C. Sapienza and J. P. Issa, *Annu. Rev. Nutr.*, 2016, **36**, 665–681.

8 F. Z. Kadayifci, S. Zheng and Y. X. Pan, *Int. J. Mol. Sci.*, 2018, **19**, 4055.

9 J. H. Park, Y. Yoo and Y. J. Park, *Prev. Nutr. Food Sci.*, 2017, **22**, 81–89.

10 J. Ying, M. H. Rahbar, D. M. Hallman, L. M. Hernandez, M. R. Spitz, M. R. Forman and O. Y. Gorlova, *PLoS One*, 2013, **8**(2), e54561.

11 P. M. Ueland, P. I. Holm and S. Hustad, *Clin. Chem. Lab. Med.*, 2005, **43**(10), 1069–1075.

12 S. A. S. Craig, *Am. J. Clin. Nutr.*, 2004, **80**(3), 539–549.

13 S. Huerta, E. J. Gaulet, S. Haerta-Yepez and E. H. Livingston, *J. Surg. Res.*, 2007, **1**, 143–156.

14 G. Zhao, F. He, C. Wu, P. Li, N. Li, J. Deng, G. Zhu, W. Ren and Y. Peng, *Front. Immunol.*, 2018, **24**(9), 1070.

15 Y. P. Du, J. S. Peng, A. Sun, *et al.*, *BMC Cancer*, 2009, **9**, 261.

16 F. Kar, C. Hacioglu, S. Kacar, V. Sahinturk and G. Kanbak, *Cell Stress Chaperones*, 2019, **24**(5), 871–881.

17 S. Sun, X. Li, A. Ren, M. Du, H. Du, Y. Shu, L. Zhu and W. Wang, *Sci. Rep.*, 2016, **6**, 35547.

18 F. Montagnani, G. Turrisi, C. Marinozzi, C. Aliberti and G. Fiorentini, *Gastric Cancer*, 2011, **14**, 50–55.

19 S. A. Fahmy, E. Preis, U. Bakowsky and H. M. Azzazy, *Materials*, 2020, **13**, 3661.

20 S. A. Fahmy, M. Alawak, J. Brüßler, U. Bakowsky and M. M. El-Sayed, *BioMed Res. Int.*, 2019, **2019**, 1–15.

21 S. El-Shafie, S. A. Fahmy, L. Ziko, N. Elzahed, T. Shoeib and A. Kakarougkas, *Pharmaceutics*, 2020, **12**, 863.

22 S. A. Fahmy and W. Mamdouh, *J. Appl. Polym. Sci.*, 2018, **135**, 46133.

23 A. Koshkaryev, R. Sawant, M. Deshpande and V. Torchilin, *Adv. Drug Delivery Rev.*, 2013, **65**, 24–35.

24 S. A. Fahmy, E. Preis, U. Bakowsky and H. M. Azzazy, *Molecules*, 2020, **25**, 4981.

25 X. J. Loh, *Mater. Horiz.*, 2014, **1**, 185–195.

26 S. A. Fahmy, J. Brüßler, M. Alawak, M. M. El-Sayed, U. Bakowsky and T. Shoeib, *Pharmaceutics*, 2019, **11**, 292.

27 S. A. Fahmy, F. Ponte, M. K. Abd El-Rahman, N. Russo, E. Sicilia and T. Shoeib, *Spectrochim. Acta, Part A*, 2018, **193**, 528–536.

28 S. A. Fahmy, F. Ponte, E. Sicilia and H. M. Azzazy, *ACS Omega*, 2020, **5**, 31456–31466.

29 S. A. Fahmy, F. Ponte, I. M. Fawzy, E. Sicilia, U. Bakowsky and H. M. Azzazy, *Molecules*, 2020, **25**, 5926.

30 D. S. Guo and Y. J. Liu, *J. Chem. Res.*, 2014, **47**, 1925–1934.

31 A. W. Coleman, S. Jebors, S. Cecillon, P. Perret, D. Garin, D. Marti-Battle and M. Moulin, *New J. Chem.*, 2008, **32**, 780–782.

32 S. A. Fahmy, I. M. Fawzy, B. M. Saleh, M. Y. Issa, U. Bakowsky and H. M. Azzazy, *Nanomaterials*, 2021, **11**, 965, DOI: 10.3390/nano11040965.

33 R. M. Allam, A. M. Al-Abd, A. Khedr, O. A. Sharaf, S. M. Nofal, A. E. Khalifa, H. A. Mosli and A. B. Abdel-Naim, *Toxicol. Lett.*, 2018, **291**, 77–85.

34 V. Vichai and K. Kirtikara, *Nat. Protoc.*, 2006, **1**, 1112–1116.

35 M. J. Frisch, G. W. Trucks, H. B. Schlegel, G. E. Scuseria, M. A. Robb, J. R. Cheeseman, G. Scalmani, V. Barone, B. Mennucci, G. A. Petersson, H. Nakatsuji, M. Caricato, X. Li, H. P. Hratchian, A. F. Izmaylov, J. Bloino, G. Zheng, J. L. Sonnenberg, M. Hada, M. Ehara, K. Toyota, R. Fukuda, J. Hasegawa, M. Ishida, T. Nakajima, Y. Honda, O. Kitao, H. Nakai, T. Vreven, J. A. Montgomery Jr, J. E. Peralta, F. Ogliaro, M. Bearpark, J. J. Heyd, E. Brothers, K. N. Kudin, V. N. Staroverov, R. Kobayashi, J. Normand, K. Raghavachari, A. Rendell, J. C. Burant, S. S. Iyengar, J. Tomasi, M. Cossi, N. Rega, J. M. Millam, M. Klene, J. E. Knox, J. B. Cross, V. Bakken, C. Adamo, J. Jaramillo, R. Gomperts, R. E. Stratmann, O. Yazyev, A. J. Austin, R. Cammi, C. Pomelli, J. W. Ochterski, R. L. Martin, K. Morokuma, V. G. Zakrzewski, G. A. Voth, P. Salvador, J. J. Dannenberg, S. Dapprich, A. D. Daniels, O. Farkas, J. B. Foresman, J. V. Ortiz, J. Cioslowski and D. J. Fox, *Gaussian 09, Revision D.01*, Gaussian, Inc., Wallingford, CT, 2009.

36 S. Grimme, *J. Comput. Chem.*, 2006, **27**, 1787–1799.

37 A. V. Marenich, C. J. Cramer and D. G. Truhlar, *J. Phys. Chem. B*, 2009, **113**, 6378–6396.

38 S. F. Boys and F. Bernardi, *Mol. Phys.*, 1970, **19**, 553.

39 R. F. W. Bader, *Chem. Rev.*, 1991, **91**, 893–928.

40 T. A. Keith, *AIMAll (Version 17.11.14)*, TK Gristmill Software, Overland Park, KS, USA, 2017, http://aim.tkgristmill.com.

41 N. J. Wheate, G. M. Abbott, R. J. Tate, C. J. Clements, R. Edrada-Ebel and B. F. Johnston, *J. Inorg. Biochem.*, 2009, **103**, 448–454.

42 D.-S. Guo, V. D. Uzunova, X. Su, Y. Liu and W. M. Nau, *Chem. Sci.*, 2011, **2**, 1722.

43 C. P. Carvalho, V. D. Uzunova, J. P. Da Silva, W. M. Nau and U. Pischel, *Chem. Commun.*, 2011, **47**, 8793–8795.

44 C. Marquez and W. M. Nau, *Angew. Chem., Int. Ed.*, 2001, **40**, 3155–3160.

45 Z. Miskolczy and L. Biczok, *J. Phys. Chem. B*, 2011, **115**, 12577–12583.

46 J. Wu and L. Isaacs, *Chem.–Eur. J.*, 2009, **15**, 11675–11680.

47 U. Pischel, V. D. Uzunova, P. Remon and W. M. Nau, *Chem. Commun.*, 2010, **46**, 2635–2637.

48 A. Praetorius, D. M. Bailey, T. Schwarzlose and W. M. Nau, *Org. Lett.*, 2008, **10**, 4089–4092.

49 A. L. Koner and W. M. Nau, *Supramol. Chem.*, 2007, **19**, 55–66.

50 L. M. Arantes, E. V. Varejao, K. J. Pelizzaro-Rocha, C. M. Cereda, E. de Paula, M. P. Lourenco, H. A. Duarte and S. A. Fernandes, *Chem. Biol. Drug Des.*, 2014, **83**, 550–559.

51 M. Shaikh, P. K. J. Mohanty, W. M. Singh and P. H. Nau, *Photochem. Photobiol. Sci.*, 2008, **7**, 408–414.

52 H. Bakirci, A. Koner, T. Schwarzlose and M. W. Nau, *Chem.–Eur. J.*, 2006, **12**, 4799–4807.

53 G. Wang, H. Zhang, F. Ding and Y. Liu, *J. Inclusion Phenom. Macrocyclic Chem.*, 2011, **69**, 85–89.

54 W. Yang and M. De Villiers, *AAPS J.*, 2005, **7**, 23, http://www.aapsj.org, accessed on 28 November 2020.

55 A. Yousaf, S. A. Hamid, N. M. Bunnori and A. A. Ishola, *Drug Des., Dev. Ther.*, 2015, **9**, 2831–2838.

56 D. Zhang, J. Zhang, K. Jiang, K. Li, Y. Cong, S. Pu, Y. Jin and J. Lin, *Spectrochim. Acta, Part A*, 2016, **152**, 501–508.

57 S. A. Fahmy, J. Brüßler, F. Ponte, M. K. Abd El-Rahman, N. Russo, E. Sicilia, U. Bakowsky and T. Shoeib, *J. Phys.: Conf. Ser.*, 2019, **1310**, 012011.